Chemical Engineering Journal 339 (2018) 259–267

Contents lists available at ScienceDirect

Chemical Engineering Journal

journal homepage: www.elsevier.com/locate/cej

Fast and efficient removal of chromium (VI) anionic species by a reusable chitosan-modified multi-walled carbon nanotube composite

Yimin Huang[a,b,c], Xinqing Lee[b,*], Florika C. Macazo[c], Matteo Grattieri[c], Rong Cai[c], Shelley D. Minteer[c,*]

[a] University of Chinese Academy of Sciences, China
[b] Institute of Geochemistry, Chinese Academy of Science, Guiyang, Guizhou 550081, China
[c] Departments of Chemistry and Materials Science and Engineering, University of Utah, 315 S 1400 E, Salt Lake City, Utah 84112, United States

HIGHLIGHTS

- A simple and cost-efficient preparation of chitosan-modified MWCNTs-COOH is shown.
- Cr (VI) removal include electrostatic adsorption and Cr (VI) reduction to Cr (III).
- Cr (VI) adsorption process is fast and efficient with 30 min equilibration time.
- Chitosan/MWCNTs-COOH composite shows reusable adsorption ability for Cr (VI).

GRAPHICAL ABSTRACT

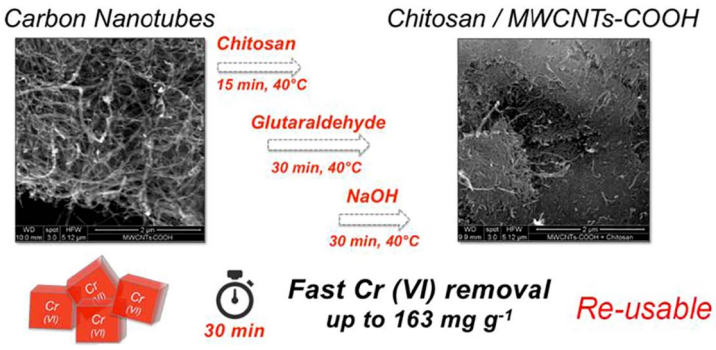

ARTICLE INFO

Keywords:
Chitosan
Carboxylated multi-walled carbon nanotubes
Chromium (VI) anionic species removal
Adsorption isotherm
Heavy metal pollution

ABSTRACT

Chromium pollution has posed an increasing problem to the aquatic environment worldwide, especially in industrial areas and mining fields. To date, the removal of Cr (VI) has been achieved by using various techniques such as chemical precipitation, solvent extraction, and electrodialysis; however, these methods typically take significantly longer reaction time and expensive, complex preparations. Herein, we demonstrate a simple polymer crosslinking method for efficient and fast removal of Cr(VI) anionic species via adsorption in aqueous solutions. Specifically, we modified carboxylated multi-walled carbon nanotubes (MWCNTs-COOH) with chitosan to enable enhanced adsorption of Cr (VI) in acidic aqueous solutions (pH = 2), resulting in maximum adsorption capacities of 142.9 ± 0.9 mg g^{-1}, 151 ± 1 mg g^{-1} and 164 ± 2 mg g^{-1} at 293 K, 303 K and 313 K, respectively. The adsorption process was exothermic, following the Langmuir isotherm model. We found that the adsorption of Cr (VI) by the composite is caused primarily through physical electrostatic adsorption as well as chemical redox reactions. Furthermore, the chitosan/MWCNTs-COOH composite was demonstrated to be successfully applicable in multiple Cr (VI) adsorption cycles, with none, or limited, loss of performance (98–100% adsorption up to the 4th cycle). Nonetheless, this chitosan-modified MWCNTs-COOH composite is capable of enhancing the adsorption capacity, as well as shortening the adsorption reaction time needed for efficient Cr (VI) removal to occur. Overall, our work presents a simple and rapid methodology in designing and fabricating new

* Corresponding authors.
E-mail addresses: lee@mail.gyig.ac.cn (X. Lee), minteer@chem.utah.edu (S.D. Minteer).

https://doi.org/10.1016/j.cej.2018.01.133
Received 7 November 2017; Received in revised form 23 January 2018; Accepted 24 January 2018

materials that will find significant utility in a number of environmental applications, such as wastewater treatment and chemical waste management.

1. Introduction

Heavy metal pollution is one of the most serious environmental problems encountered by many areas on a daily basis. Extensive involvement of heavy metals in industries such as mining, smelting and refining of Cr-bearing minerals has posed a threat to the quality of the aquatic environment and soils [1]. Cr normally exists as Cr (III), based on valency, in the form of $Cr(OH)^{2+}$, $Cr(OH)_3^0$ and $Cr(OH)_4^-$, or as Cr (VI) in the species of $HCrO_4^-$, CrO_4^{2-} and $Cr_2O_7^{2-}$ [2]. Cr (VI) is 500 times more toxic than Cr (III) and has been reported as a major cause of various health problems, such as lung cancer, skin irritation, and kidney, liver and stomach damage [3]. To avoid the harmful effects of Cr, the maximum allowable Cr (VI) concentration should not exceed 0.05 mg L^{-1} in drinking water, as recommended by the World Health Organization (WHO) and American Water Works Association (AWWA) [4]. At the same time, the accumulative release of Cr (irrespective of its species) from potential Cr dischargers should not surpass the legal limits of 50 mg L^{-1} in drinking water [4] or 100 mg L^{-1} in surface waters, as specified by the US Environmental Protection Agency (EPA) [5].

To abide with the federal regulations, techniques have been developed recently for removal of Cr from aqueous environments. These include chemical precipitation, flotation, reduction, ion exchange, electrodialysis, solvent extraction, biosorption, and membrane separation, among others [6,7]. Many of these methods proved disadvantageous in terms of economic cost, chemical reagents, and inability to comply with the EPA requirements. Conversely, sorption has shown superior advantages like low initial cost, water recycling, environmentally-friendly, and simplicity in utility operation over current removal techniques [8]. This is especially the case for carbon-based adsorbents, which are often environmentally-friendly and cost-effective [3].

As a newer member of the carbon family, carbon nanotubes (CNTs) are characterized by nanometer-scale diameter sizes, large surface area, high mechanical strength, remarkable electrical conductivity and relatively low cost, making them attractive materials for use in different applications [9–12]. As a result, CNTs have been recognized for their high adsorption capabilities, [13] and thus, have been widely studied as a promising adsorbent alternative for wastewater treatment [3] and removal of metallic pollutants in the environment [14]. More so, it has been demonstrated that the adsorption capacity of CNTs can further be enhanced via chemical treatment or modification with chitosan [15–22].

Chitosan is an environmentally-friendly and naturally abundant cationic biopolymer. It is produced industrially through alkaline N-deacetylation of chitin, the main component of the shells of crab, shrimp and krill, and is commercially available at low prices. Chitosan's high hydrophilicity, owing to a large number of hydroxyl groups in its glucose units, as well as functional groups such as acetamido, primary amino and/or hydroxyl groups in its structure, is supposedly useful for heavy metal adsorption and anion-polluted-water treatment [23]. Previous studies, however, showed that it was rather inefficient in Cr (VI) adsorption, [24] because its 3D-ordered structure renders preferential adsorption of the metal ions in the amorphous region, and thus, restricts the ability of anion adsorption [25]. The adsorption ability was significantly improved by associating with multi-walled carbon nanotubes (MWCNTs) [26] or other materials like organoclay [23]. Different drawbacks still characterized these studies, i.e. the complexity involved in the process of modification and the long reaction time to reach the adsorption equilibrium [27,23,13,28]. To overcome these problems, a simple crosslinking method was developed in this study. By modifying MWCNTs-COOH with chitosan, we created a chitosan/MWCNTs-COOH composite capable of fast and efficient removal of Cr (VI) anionic species in aqueous solution. Compared to the previous reports, our strategy considerably shortened the reaction time, as well as simplified the steps needed for the preparation of the composite, while significantly improving the overall adsorption of Cr(VI) in acidic aqueous solutions. The mechanism of the Cr (VI) removal is also discussed, since we found that both sorption and reduction processes were involved in the process.

2. Materials and methods

2.1. Chemicals and materials

MWCNTs-COOH (30–50 nm in diameter) were obtained from Cheap Tubes Co. Ltd. (Cambridgeport, VT). Chitosan (CS, MW: 310–375 kDa), potassium dichromate and glutaraldehyde were purchased from Sigma-Aldrich (St. Louis, MO) and used as received. All reagents used in this work were of analytical grade. All solutions were prepared in ultrapure water (18.25 MΩ cm^{-1}) using a Millipore Milli-Q ultrapure water purification system.

2.2. Preparation of chitosan/MWCNTs-COOH composite

1 g of chitosan (CS) was dissolved in 400 mL of 2% (v/v) acetic acid and heated at 40 °C. To this solution, 1 g of MWCNTs-COOH was added and the mixture was stirred for 15 min at 40 °C. 0.4 mL of glutaraldehyde was then injected into the reaction system with continuous stirring, while maintaining the solution temperature at 40 °C. After 30 min, 1 L ultrapure water was added into the mixture, followed by 120 mL of 0.10 M NaOH and stirred for 30 min. Finally, the mixture was cooled to room temperature for 15 min, and excess water was removed using a pipette to achieve a sponge-like mixture made of MWCNTs-COOH. The samples were oven dried (80 °C) for 12 h, and sieved through a 100-mesh screen.

2.3. Characterization of chitosan/MWCNTs-COOH composite

The morphologies of MWCNTs-COOH and chitosan/MWCNTs-COOH composite were characterized using scanning electron microscopy (SEM, FEI Quanta 600F), the surface chemistries were analyzed via X-ray photoelectron spectroscopy (XPS, Kratos Axis Ultra DLD system) using monochromatic Al Kα X-ray source and a spot diameter of 400 mm. pH_{pzc} of MWCNTs-COOH and Chitosan/MWCNTs-COOH were determined by WMOB-06 through zeta-potential analysis, and the total Cr present in solution was analyzed using an inductively coupled plasma-mass spectrometry (ICP-MS, Agilent 7500ce).

2.4. Adsorption and kinetic experiments

The adsorption experiments were carried out in 250 mL flasks, where 50 mg of the adsorbent was added to 50 mL of Cr (VI) solution unless otherwise stated. The reaction mixtures were shaken using a rotary shaker at 150 rpm. The effect of pH on Cr (VI) adsorption by chitosan/MWCNTs-COOH and MWCNTs-COOH was first studied by varying the pH of the solution from 2.0 to 8.0. Subsequent adsorption experiments were then performed at the optimum pH (*vide infra*) and at temperatures of 293 K, 303 K, and 313 K. The concentration of Cr (VI) was varied from 50 mg L^{-1} to 600 mg L^{-1} and the equilibrium time was

set to 24 h. Adsorption kinetic experiments were done using Cr (VI) concentrations of 50, 100, and 200 mg L^{-1} (pH = 2.0), where measurements were taken at varying time points (5–1440 min). In addition, the effect of background anion on the adsorption of Cr (VI) was studied using separate 0.01 M solutions of NaCl, KNO_3, KH_2PO_4 and Na_2SO_4 added to the composite.

To determine the amount of Cr(VI) in the residual solution, the reacted samples were filtered through a 0.45 μm microporous membrane and Cr(VI) concentration was determined by UV–Vis spectroscopy at 540 nm (Evolution 260 Bio UV–Vis spectrophotometer, Thermo Scientific).

The amount of Cr (VI) adsorbed per unit mass of the adsorbent was quantified using the mass balance equation as follows:

$$q_e = \frac{V(C_0 - C_e)}{m} \quad (1)$$

where q_e is the adsorption capacity (mg g^{-1}), C_0 and C_e are the initial and equilibrium concentration (mg L^{-1}) of Cr (VI) respectively, V is the volume (L) of solution and m is the weight (g) of adsorbent.

2.5. Desorption experiments

To demonstrate the reusability of the chitosan/MWCNT's-COOH composite for the removal of Cr (VI), 0.1 M NaOH was used as the desorption solution. Briefly, 500 mg of the chitosan/MWCNTs-COOH composite was added to 500 mL of 200 mg L^{-1} Cr solution, and shaken for 2 h at 303 K to adsorb Cr(VI). The mixture was filtered and washed six times with ultrapure water, then mixed with 500 mL of 0.10 M NaOH solution and shaken for 2 h at 303 K to desorb Cr(VI) from the composite. The mixture was filtered and washed again six times with ultrapure water. The adsorption capacity was calculated using Eq. (1).

3. Results and discussion

3.1. Characterization of MWCNTs-COOH and chitosan/MWCNTs-COOH composite

SEM micrographs show that MWCNTs-COOH exhibited fibrous morphology (Fig. 1, a), and the fibers could clearly be distinguished. When modified with chitosan, the resulting composite appeared more homogenous and smoother (Fig. 1b), with MWCNTs-COOH fibers protruding out of the surface of chitosan.

The XPS analysis reveals two significant peaks, C 1s and O 1s, at the surface of MWCNTs-COOH (Fig. 2, left, black curve). After treatment with chitosan, a small N 1s peak appeared in the spectra obtained for the chitosan/MWCNTs-COOH composite (Fig. 2, left, red curve; Fig. 2, left, inset). XPS analysis of the chitosan-modified composite before (Fig. 2, right, black curve) and after (Fig. 2, right, red curve) adsorption of Cr (VI) also show a N 1s peak indicative of the presence of amino groups and a Cr 2p peak (~575–580 eV), demonstrating successful modification of the MWCNTs-COOH with chitosan, as well as efficient adsorption of Cr (VI) by the composite. Moreover, detailed XPS analysis of Cr shows the presence of Cr (III) (5 peaks in total including the main peak at ~576 eV) and Cr (VI) (broad peak at ~579 eV and ~580 eV) [29] on the surface of the composite (Fig. 2, right, inset). However, the initial solution only contained hexavalent Cr, thus, some of the Cr (VI) species have been reduced to Cr (III) during the adsorption process. A summary of the calculated percent compositions of C, N, O, and Cr on the surface of the composites (Table 1) further support these results, as the N 1s peak increased by 0.7% after treatment with chitosan, while the percentage of Cr was found to be ~1.1% (Table 1) on the surface of the chitosan/MWCNTs-COOH composite after adsorption of Cr (VI). The amount of Cr (VI) loaded on the surface of the composite is lower than the removed amount from the solution (51 mg g^{-1} for the solution of 100 mg L^{-1} Cr(VI) at pH2). This is because 1). the Chitosan/MWCNTs-COOH composite was washed with water at pH 5 before the analysis, possibly reducing the sorption capacity and 2). part of the Cr (III) reduced from Cr(VI) still exists in the solution. After adsorption of Cr (VI), N on the Chitosan/MWCNTs-COOH was increased from 0.7% to 1.5% (Table 1), rather than being reduced by addition of Cr (VI) as expected. This is probably a result of uneven distribution of chitosan on the surface of the MWCNTs.

Further analysis is conducted based on the deconvolution of C1s XPS spectra of chitosan/MWCNTs-COOH. The C1s peak is deconvoluted into four main fitting curves with peaks at 284.5, 285.9, 286.7 and 288.4 eV, which correspond to C—C, C—O, C═O, O—C═O, respectively (Fig. 3). The percentage of C—C decreased after Cr(VI) adsorption, while that of the oxygen-related functional groups C—O, C═O and O—C═O increased (Table 2). After desorption of Cr, the percentage of carbon-related groups on chitosan/MWCNTs-COOH remains in the same ball park. The deconvolution analysis of N1s XPS spectra of chitosan/MWCNTs-COOH also shows that N—H- decreased significantly after the adsorption. Meanwhile, a new peak appeared at around 402.0 eV, which is indicative of the group $=NH^+$- (Fig. 3). All these results suggested that the chitosan/MWCNTs-COOH has been oxidized significantly after the adsorption of Cr(VI).

3.2. Mechanism of Cr (VI) removal

ICP-MS analysis was also performed, revealing the presence of a small amount of Cr(III) in the solution (in the order of 6–12 mg L^{-1}), obtained as the difference between the concentration of total Cr and the concentration of Cr(VI) detected by UV–vis. Moreover, the reduction of Cr (VI) to Cr (III) is suggested by XPS results, with the oxidation of C—C, obtaining C—O, C═O and O—C═O, and the oxidation of N—H- to $=NH^+$-. Therefore, the reduction mechanism could be explained by the fact that at pH 2.0 large amounts of H^+ could lead to the protonation of N—H-, formation of more oxygenated groups on chitosan/MWCNTs-

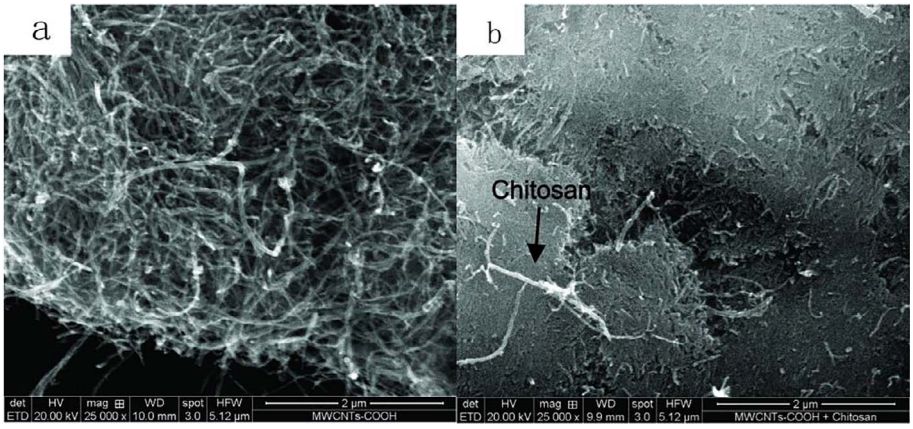

Fig. 1. SEM micrographs of MWCNTs-COOH (left) and chitosan/MWCNTs-COOH composite (right).

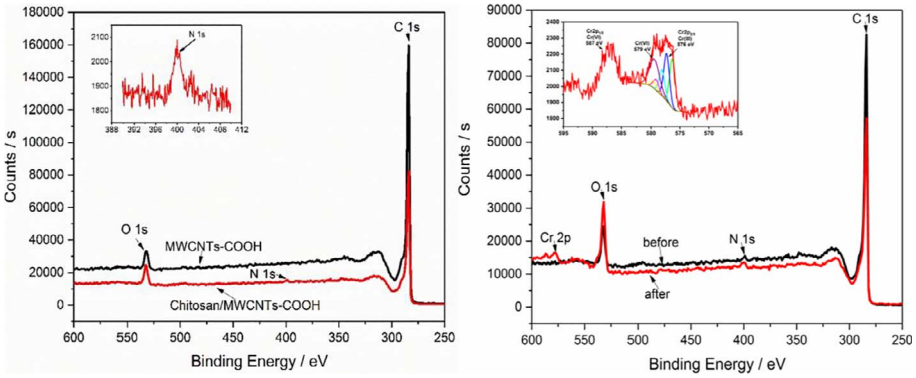

Fig. 2. (Left) XPS spectra obtained for MWCNTs-COOH (black curve) and chitosan/MWCNTs-COOH composite (red curve). The inset shows a zoomed in region of the N 1s peak for the chitosan-modified composite. (Right) XPS spectra obtained for chitosan/MWCNTs-COOH composite before (black curve) and after (red curve) adsorption of Cr (VI). The inset shows a zoomed in region of the Cr 2p peaks for the Cr adsorbed on the composite. (For interpretation of the references to colour in this figure legend, the reader is referred to the web version of this article.)

Table 1
Surface elemental composition.

Adsorbent	% Composition			
	C	O	N	Cr
MWCNTs-COOH	97.2	2.8		
Chitosan/MWCNTs-COOH	94.0	5.3	0.7	
Chitosan/MWCNTs-COOH/Cr	88.1	9.8	1.5	1.1

Table 2
Relative atomic percent of carbon and nitrogen components.

Chitosan/MWCNTs-COOH	C–C	C-O	C═O	COO	NH-	NH^+-
Before adsorption	74.4	9.8	6.4	4.7	92	——
After adsorption	63.5	10.6	16.4	7.2	76.6	23.4
After desorption	60.1	13.5	15.8	7.5	83.9	16.1

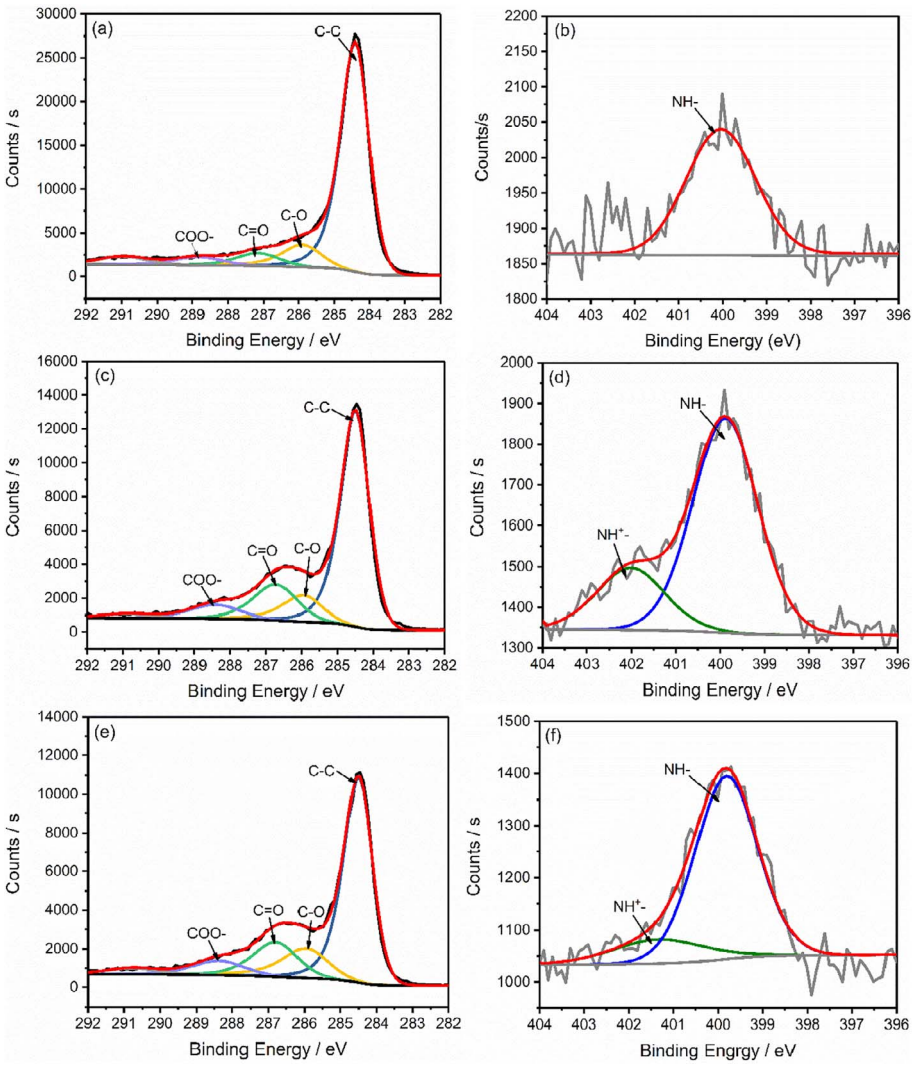

Fig. 3. Results of XPS spectra analysis. (a) the C 1s XPS spectra of chitosan/MWCNTs-COOH before and (c) after adsorption, and (e) after desorption. (b) the N 1s XPS spectra of chitosan/MWCNTs-COOH before and (e) after adsorption, and (f) after desorption.

COOH and the reduction of Cr(VI) to Cr(III) as represented by the following Eq. (2):

$$HCrO_4^- + 7H^+ + 3e \leftrightarrow Cr^{3+} + 4H_2O \quad (2)$$

The adsorption of Cr (VI) by the chitosan/MWCNTs-COOH composite involves three mechanisms, including both physical electrostatic adsorption and chemical redox reactions [30,31]. This was schematized in Fig. 4. Physical electrostatic adsorption is caused by the strong electrostatic interaction between the negatively charged Cr (VI) anionic species and the positively charged protonated amine and carboxylated groups at the surface of the composite (Fig. 4a). In this process, a chemical redox reaction also occurs when some of the Cr (VI) bound to the protonated amine and carboxylated groups are reduced to Cr (III), which are then desorbed from the composite and released into the solution due to electrostatic repulsion (Fig. 4b). Finally, a second chemical redox reaction can possibly occur via the direct reduction of free Cr (VI) anionic species to Cr (III), where the latter are subsequently adsorbed by the chitosan/MWCNTs-COOH composite (Fig. 4c). This also explains the presence of Cr (III) species in the composite as shown in the XPS analysis above (Fig. 2, right). pH of the solution and initial Cr (VI) concentration significantly affects the occurrence of physical electrostatic adsorption and chemical redox reactions between the Cr (VI) anionic species and the composite. When the pH is lower than the net charge of the adsorbent, more protons are available in solution, which significantly protonate the amine and carboxylated groups of the composite. This, in turn, promotes physical electrostatic adsorption, and thus, removal of the Cr (VI) species onto the now positively charged surface of the composite. A large amount of protons also promote the reduction of Cr (VI) into Cr (III) [31,32]. Furthermore, electrostatic adsorption increases with an increase in the initial concentration of Cr (VI), owing to an increased probability of contact between the Cr (VI) species and the positively charged groups on the adsorbent. Park et al. [30] and Liu et.al [31] also reported that the reduction of Cr (VI) to Cr (III) could be enhanced with an increase in the initial Cr (VI) concentration.

3.3. Effect of solution pH

Since the pH of the solution is an important factor in optimizing the conditions for efficient adsorption of Cr (VI), we first studied the effect of pH on our working solutions and determined the best pH to use for the rest of the adsorption and kinetic experiments. Solution pH generally influences the surface charge of the adsorbent, as well as the ionization degree of the materials in solution, [33] thereby affecting the overall ability of the chitosan-modified composite to adsorb or remove Cr(VI) in aqueous solution. Fig. 5 shows the result of adsorption by MWCNTs-COOH (Fig. 5, left, black curve) and chitosan/MWCNTs-COOH composite (Fig. 5, left, red curve) at varying pHs. As shown, the adsorption of Cr (VI) by chitosan/MWCNTs-COOH decreased from ~57% to ~0% as the pH increased from 2 to 8. Meanwhile, the adsorption by MWCNTs-COOH decreased from ~ 6% to ~0% as the pH varies from 2 to 8. In both cases, an acidic environment is preferred for effective Cr (VI) adsorption, where the maximum adsorption was achieved at pH 2.0. Moreover, it is evident that the pH affects the adsorption ability of the chitosan/MWCNTs-COOH composite more than the MWCNTs-COOH alone.

The observed decrease in Cr (VI) adsorption with increasing pH can be explained as a result of competitive adsorption induced by OH^-. The amount of OH^- ions increase with pH, which compete substantially with CrO_4^{2-} for adsorption sites. On the other hand, pH is also associated with the net electric charge of the solution, as shown in Fig. 5 (right). The MWCNTs-COOH and Chitosan/MWCNTs-COOH solution

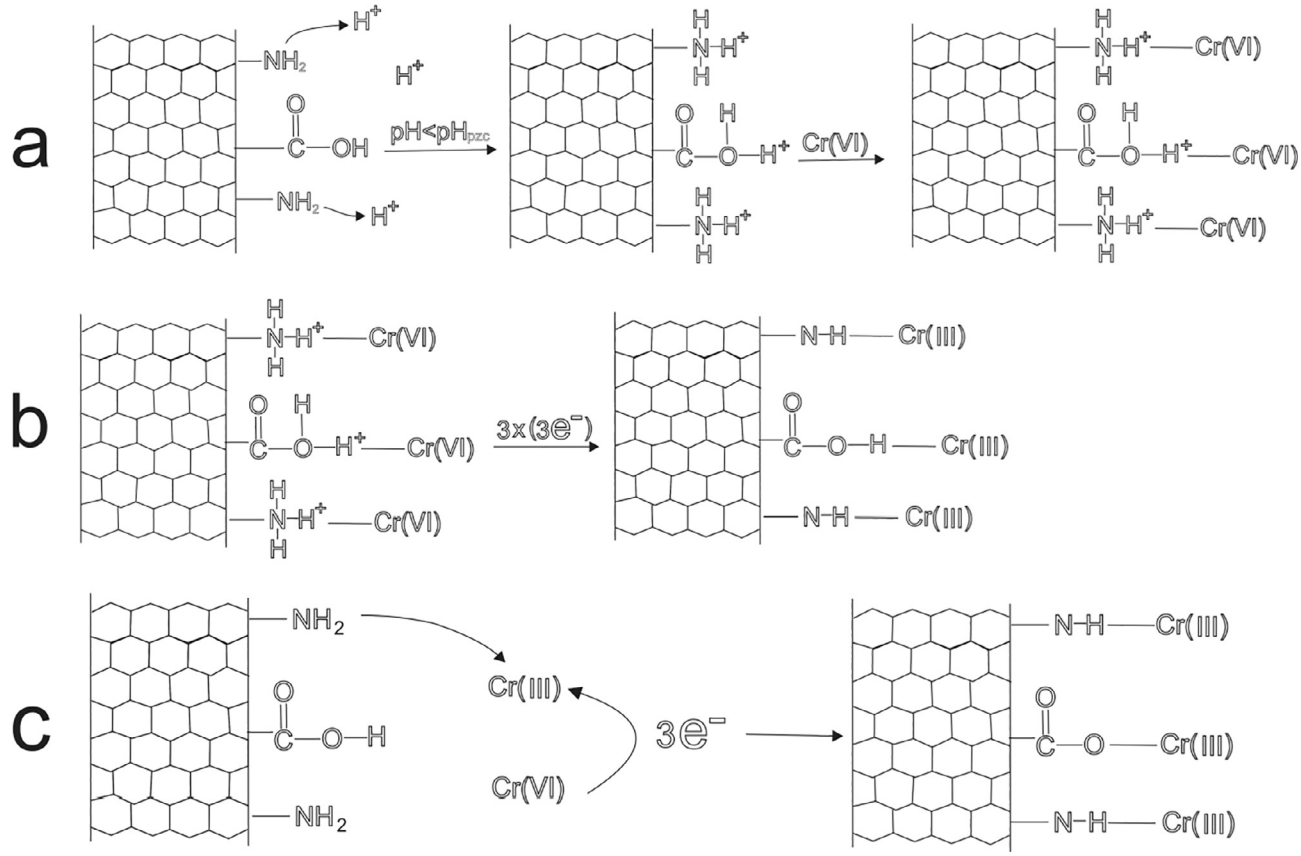

Fig. 4. Three adsorption mechanisms proposed for the removal of Cr (VI) by the chitosan/MWCNTs-COOH composite. (a) Physical electrostatic adsorption involving the interaction between the positively charged amine and carboxyl groups at the surface of the composite and Cr (VI); (b) the first chemical redox reaction where bound Cr (VI) is reduced to Cr (III); and (c) the second chemical redox reaction where free Cr (VI) in solution is reduced to Cr (III) first followed by adsorption of the Cr (III) by the composite.

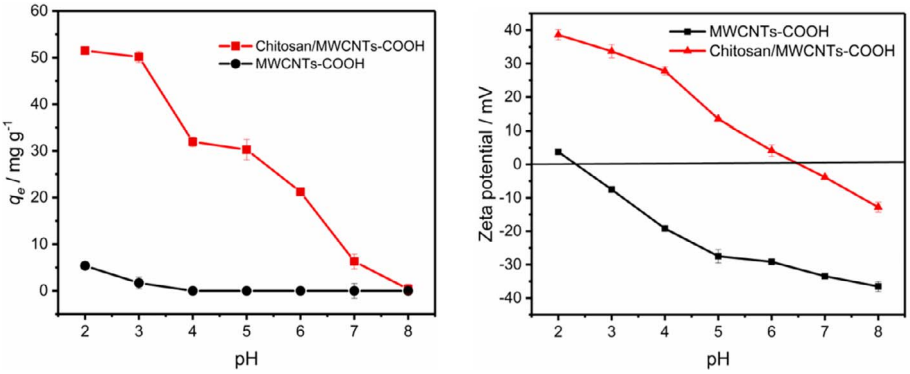

Fig. 5. (left) Effect of pH on the adsorption of Cr (VI) on MWCNTs-COOH (black curve) and chitosan/MWCNTs-COOH composite (red curve). Adsorption experiments were carried out at 303 K using an adsorbent dose of 0.05 g and a concentration of 100 mg L^{-1} in a 50 mL solution. (right) Zeta potential of MWCNTs-COOH (black curve) and chitosan/MWCNTs-COOH (red curve). (For interpretation of the references to colour in this figure legend, the reader is referred to the web version of this article.)

has a zero charge occurring at pH 2.3 and 6.5. At pH's lower than 6.5, the surface of Chitosan/MWCNTs-COOH would be positively charged, while negatively charged at pH's greater than 6.5. These pH-induced changes in electric charge consequently influence the adsorption of Cr (VI) species on the surface of the chitosan-modified nanotube composite [34]. However, as shown in Fig. 5 (left), Chitosan/MWCNTs-COOH still remove small amounts of Cr(VI) from the aqueous solution at pH 7($> pH_{pzc}$). Moreover, the XPS analysis of Chitosan/MWCNTs-COOH after treatment by the Cr(VI) solution at pH 7 revealed that the percentage of C—C decreased while NH^+- increased (Supporting Information, Fig. S2). Both indicated the mechanism of Cr(VI) removal is a chemical redox reaction at the solution of pH 7.

The effect of pH on the adsorption ability of the composite can also be explained thermodynamically. The varying adsorptive capacities at different pH's may be related to the adsorption free energies of various chromium species (i.e. $HCrO_4^-$, H_2CrO_4 and CrO_4^{2-}) existing at different pH's. For instance, at pH 1.0–3.0, $HCrO_4^-$ is the predominant species in solution, [35] which is gradually replaced by CrO_4^{2-} as pH increases. The adsorption free energy of $HCrO_4^-$ is lower than that of CrO_4^{2-}, hence, $HCrO_4^-$ is more favorably adsorbed than CrO_4^{2-} at the same concentration [36]. In addition, at low pH, large amounts of protons have a positive effect for promoting the reduction of Cr (VI) to Cr (III), thus reducing the Cr (VI) anionic species in the solution [29]. Overall, pH of the solution plays an important role for the fast and effective removal of Cr (VI).

3.4. Effect of contact time and kinetics of the adsorption

In addition to pH, contact time, or the amount of time that the adsorbent was incubated with Cr (VI), was also found to markedly affect the adsorption of Cr (VI) anionic species. As shown in Fig. 6, the removal capacity of chitosan/MWCNTs—COOH drastically increased in the first 10 min of contact, especially at high Cr (VI) concentrations (~200 mg L^{-1}), and then steadily increased until the adsorption equilibrium was reached, which was ~ 30 min. Of note, only data from 0 to 120 min is shown in Fig. 6 to better demonstrate the increase in adsorption capacities during the first 30 min (the point of saturation), although data points were collected up to 1440 min. These results can be due to the fact that at the beginning of the experiment, there were plenty of available active sites on the adsorbent surface, thus facilitating adsorption of Cr (VI). Over time, the active sites were mostly occupied by Cr (VI) until the point of saturation, thereby slowing down the adsorption process beyond the saturation point [37].

In order to quantify these experimental observations, we calculated relevant kinetic parameters that can describe the kinetics of the adsorption reactions. The pseudo-first order and pseudo-second order models are often used to evaluate the kinetics of adsorption [6,38] using the following equations [28,38,39]:

$$q_t = q_e(1-exp(-k_1 t)) \quad (3)$$

$$\frac{t}{q_t} = \frac{1}{K_2 q_e^2} + \frac{t}{q_e} \quad (4)$$

where q_t (mg g^{-1}) and q_e (mg g^{-1}) are the adsorption capacities of metal ions at time t (min) and equilibrium time (min), respectively, while k_1 (min^{-1}) and k_2 (g mg^{-1} min^{-1}) are the pseudo-first-order and pseudo-second order rate constants, respectively.

Comparing the values obtained using both models, it is evident that the R^2 values obtained using the pseudo-second order model are higher than the values obtained using the pseudo-first order model, and that the q_e^{exp} values agree well with the q_e^{cal} using the pseudo-second order model (Supporting Information, Table S1). Both parameters strongly suggest that the adsorption process of Cr (VI) by chitosan/MWCNTs-COOH composite follows a pseudo-second order model even at different concentrations (Supporting Information, Fig. S1). The pseudo-second order kinetics model is based on the assumption that the chemisorption process is the rate-limiting step. Therefore, the adsorption of Cr (VI) by chitosan/MWCNTs-COOH can then be assumed to be controlled by a chemical process, and that adsorption and reduction occurred during Cr (VI) removal [40].

3.5. Adsorption isotherms

To further characterize the adsorption process, we constructed adsorption isotherms based on studies we performed at different temperatures and varying equilibrium concentrations of the adsorbate

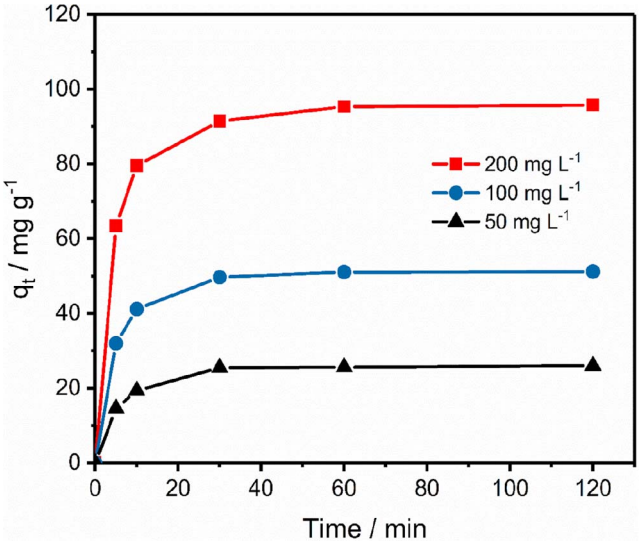

Fig. 6. Effect of contact time on Cr (VI) adsorption using concentrations at 50 mg L^{-1} (black curve), 100 mg L^{-1} (blue curve), and 200 mg L^{-1} (red curve). Adsorption experiments were carried out at 303 K using an adsorbent dose of 0.05 g in a 50 mL solution (pH = 2.0). (For interpretation of the references to colour in this figure legend, the reader is referred to the web version of this article.)

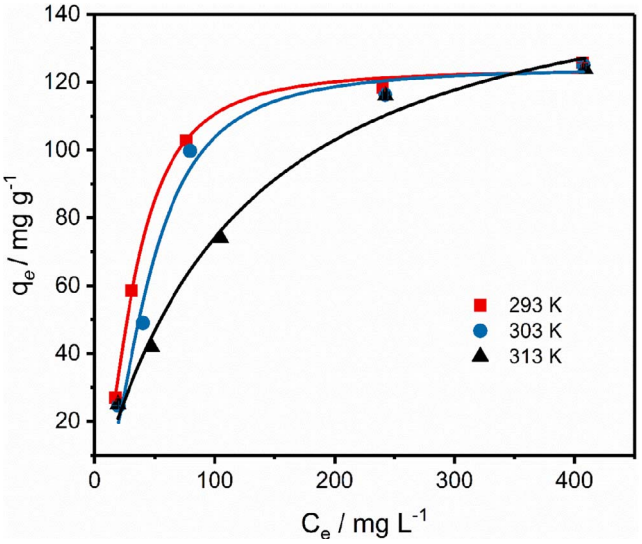

Fig. 7. Langmuir isotherm for the adsorption of Cr (VI) on chitosan/MWCNTs-COOH composite. Adsorption experiments were carried out at 293 K (red curve), 303 K (blue curve), and 313 K (black curve) using an adsorbent dose of 0.05 g and concentrations from 50 to 600 mg L^{-1} in a 50 mL (pH = 2.0) solution. (For interpretation of the references to colour in this figure legend, the reader is referred to the web version of this article.)

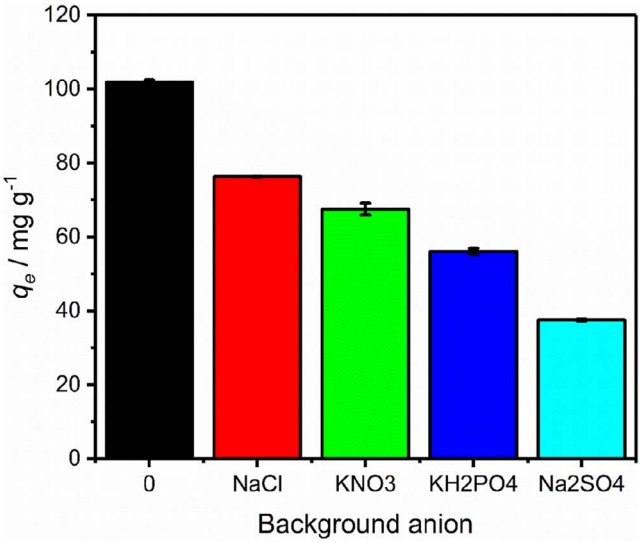

Fig. 8. Effect of background anion on Cr (VI) adsorption on chitosan/MWCNTs-COOH composite. Adsorption experiments were carried out using NaCl (red), KNO_3 (green), KH_2PO_4 (blue), and Na_2SO_4 (blue green) at 303 K using an adsorbent dose of 0.05 g and concentration of 200 mg L^{-1} in a 50 mL (pH = 2.0) solution. (For interpretation of the references to colour in this figure legend, the reader is referred to the web version of this article.)

under analysis [6]. As shown in Fig. 7, the sorption capacity was consistently reduced with increasing temperature from 293 K (Fig. 7, red curve) to 303 K (Fig. 7, blue curve) to 313 K (Fig. 7, black curve) and at varying Cr (VI) concentrations of 50, 100 and 200 mg L^{-1}. Notably, because the reaction is exothermic (*vide infra*), high temperatures decreased the overall rate of reaction, hence, the adsorption capacity of Cr (VI) (Fig. 7, blue and black curves). However, the variation of the sorption capacity with temperature become negligible for high concentrations of the contaminants (400 mg $L^{-1}$and 600 mg L^{-1}), which favorably promote electrostatic adsorption, as well as by concomitant reduction of Cr (VI). Thus, the results indicate that temperature affects the adsorption process mostly at low Cr (VI) concentrations (< ~300 mg L^{-1}).

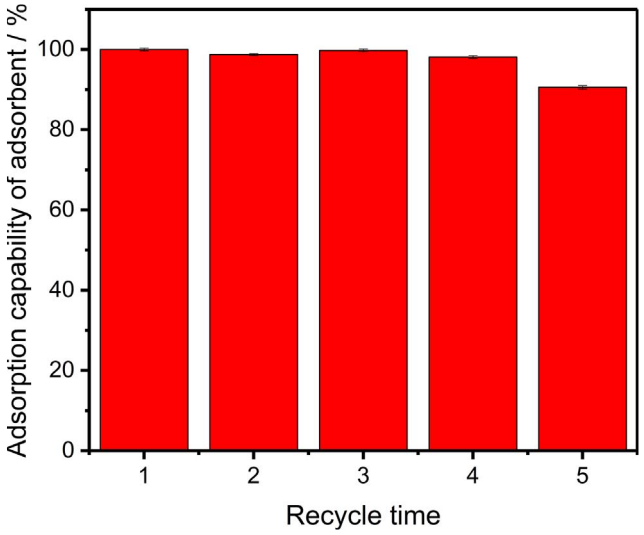

Fig. 9. Effect of recycle time on the adsorption performance of chitosan/MWCNTs-COOH composite. Adsorption capabilities calculated for the 2nd–5th cycle were normalized to the first adsorption capacity and expressed as percentage (%) adsorption capacity. Adsorption experiments were carried out at 303 K using an adsorbent dose of 0.5 g in a 500 mL solution (pH = 2.0).

Langmuir and Freundlich isotherms are often used to better understand adsorption processes. The former assumes a monolayer coverage of adsorbate over a homogeneous adsorbent surface, and that the adsorption of each molecule onto the surface has equal adsorption activation energy. The latter considers a heterogeneous surface with a non-uniform distribution of adsorption heat over the surface and that a multilayer adsorption can be formed [41].

The Langmuir and Freundlich isotherms are mathematically expressed in terms of concentrations and adsorption capacities as shown in Eqs. (5) and (6), respectively:

$$\frac{C_e}{q_e} = \frac{1}{K_L q_m} + \frac{1}{q_m} C_e \quad (5)$$

$$\ln q_e = \ln K_F + \frac{1}{n} \ln C_e \quad (6)$$

where q_m is the maximum amount of adsorption (mg g^{-1}), K_L is the adsorption equilibrium constant (L mg^{-1}), C_e is the equilibrium concentration of substrates in the solution (mg L^{-1}), K_F is a constant representing adsorption capacity, and n is a constant depicting the adsorption intensity. Of note, the Freundlich model indicates a favorable physical process if the value of (1/n) is close to zero, as well as if n is higher than unity [42].

Using these 2 models, we calculated relevant adsorption isotherm parameters (Supporting Information, Table S2), which clearly show that the Langmuir isotherm model fits the experimental results better than the Freundlich model, suggesting that the energies of the active sites on the surface of chitosan/MWCNTs-COOH composite are similar. The calculated maximum Cr (VI) adsorption capacity also increased from 142.86 mg g^{-1} ± 0.89 to 163.93 ± 1.88 mg g^{-1} at temperatures of 293 K, 303 K and 313 K.

A comparison of q_{max} values for Cr (VI) adsorption by chitosan/MWCNTs-COOH with those reported previously using different absorbents reveal that the removal capacity of chitosan/MWCNTs-COOH was higher than many other adsorbents, such as carbon nanotubes [28,42–45] and chitosan-modified adsorbents [23,44,46,47] among others [39,44,48,49] (Supporting Information, Table S3). Notably, the removal capacities of MnO_2/Fe_3O_4/o-MWCNTs and chitosan-biochar/γ-Fe_2O_3 [37,50] were higher than chitosan/MWCNTs-COOH, although their modification procedures were more complicated and required longer equilibrium times (~2–6 h) compared to the current

methodology reported. Furthermore, Hu et al. found that 100% Cr (VI) is removed from solution and adsorbed onto oxidized MWCNTs after 280 h [28]. Pillay et al., on the other hand, observed that the equilibrium is only attained after 12 h of contact time [13]. Lu et al. and Huang et al. both observed that the Cr (VI) sorption reached a plateau after about 10 h [51,52]. Finally, Kumar et al. reported an the equilibrium time of 9 h, [45] while Ansari et al. observed an equilibrium time of 8 h [53]. In summary, all the adsorption times that were previously reported are generally higher than the equilibration time (~30 min) reported in our current work. Therefore, chitosan/MWCNTs-COOH has a great potential in dealing with Cr (VI) pollution in aquatic environments.

Another factor to consider in developing novel adsorbent materials is the cost. The current market price of MWCNTs is $20 per gram ($/g), which is higher than other potential adsorbents such as activated carbon ($0.08/g), synthetic resin ($3/kg–$25/kg), and agricultural waste ($100/t). However, improved manufacturing techniques, such as chemical vapor deposition (CVD) and mass production have substantially reduced the costs when compared to $200/g of adsorbent decades ago. CVD is considered a promising technique to reduce the cost of MWCNTs in the future and, thus, increases the potential of CNTs in practical applications [54].

3.6. Thermodynamics studies

We also calculated thermodynamic parameters (i.e. standard free energy change (ΔG^o), enthalpy change (ΔH^o) and entropy change (ΔS^o)) to evaluate the spontaneity of the adsorption process (Supporting Information, Table S4). Our calculations show that the value of ΔG° ($-16.93\ kJ\ mol^{-1}$) became less negative with rising temperature, indicating that the adsorption was spontaneous and that the degree of spontaneity was reduced by increasing temperatures. The negative value of ΔH° ($-33.30\ kJ\ mol^{-1}$) indicates that the adsorption was exothermic, while the negative value of ΔS° ($-0.056\ kJ\ K^{-1}\ mol^{-1}$) shows that while Cr (VI) was adsorbed on the adsorbents, the degree of disorder decreased at the solid/solution interface. These results are consistent with the literature, which reports that the adsorption of Cr (VI) is a spontaneous and exothermic process [37].

3.7. Effect of background anion on Cr (VI) removal

We also studied the effect of background anions on the ability of the chitosan/MWCNTs-COOH composite in adsorbing Cr (VI). Fig. 8 summarizes the results when the composite was tested in the presence of NaCl (Fig. 8, red curve), KNO_3 (Fig. 8, green curve), KH_2PO_4 (Fig. 8, blue curve), and Na_2SO_4 (Fig. 8, blue green curve). Compared to an adsorption capacity of $101.85 \pm 0.57\ mg\ g^{-1}$ obtained in the absence of competing anions (Fig. 8, black curve), the adsorption capacity was reduced to $76.29 \pm 0.09\ mg\ g^{-1}$, $67.52 \pm 1.61\ mg\ g^{-1}$, $56.11 \pm 0.80\ mg\ g^{-1}$ and $37.51 \pm 0.24\ mg\ g^{-1}$ in solution containing NaCl, KNO_3, KH_2PO_4 and Na_2SO_4, respectively. As Cl^- and NO_3^- are monovalent anions, their competition with the chromium anions for the positively-charged sorption sites on the surface of chitosan/MWCNTs-COOH was relatively small. PO_4^{3-} and SO_4^{2-} however, are multivalent anions, thus competing more aggressively with Cr (VI) for the positively-charged sorption sites. [37]

3.8. Desorption studies

The ability of an adsorbent to desorb particulates (which we refer to herein as the “composite reusability”) is a key parameter in assessing its potential for real-world applications, since it will not only reduce the overall cost, but also enable the recovery of metals extracted from aqueous solutions [14]. Hence, an ideal and functional adsorbent should have higher adsorption capacity, as well as reusable performance [3]. To demonstrate the reusability of our chitosan/MWCNT's-COOH composite, we carried out adsorption-desorption experiments that were cycled five times and calculated the adsorption capacities as shown in Fig. 9. It is evident that the adsorption performance of the composite remained essentially unchanged up to the 4th cycle (~98–100%), although the adsorption capacity slightly decreased to ~91% on the 5th cycle. This could be attributed to the effect of 0.10 M NaOH, which partially weakened the reactivity of some of the active sites of the adsorbent.

4. Conclusions

In this study, we describe the development of a rapid and simple methodology of modifying the surface of MWCNTs-COOH with amino group-rich chitosan for the effective and fast removal of Cr (VI) in aqueous solution. Key advantages of this technique include increased adsorption capacity, shortened adsorption reaction time, as maximum adsorption capacities ($143–164\ mg\ g^{-1}$) were easily achieved within only 30 min, and reusability of the composite for Cr (VI) removal in aqueous solution. Our data revealed that the mechanism involved in the adsorption of Cr (VI) includes physical electrostatic adsorption via the positively charged amine and carboxyl groups on the surface of the composite at low pH, as well as subsequent reduction of Cr (VI) to Cr (III), leading to the fast and efficient removal of Cr (VI) in solution. An increase in temperature and acidity of the solution were advantageous to the adsorption process, which was both exothermic and spontaneous, thus, following a pseudo-second order equation and the Langmuir isotherm model. A limited competitive adsorption was also observed in the presence of Cl^- and NO_3^- anions, which further increased in the presence of PO_4^{3-} and SO_4^{-2}. Overall, we demonstrate that chitosan/MWCNTs-COOH composite is a promising adsorbent for the treatment of Cr pollution in aquatic environments, and its reusability is of extreme relevance in field applications. Future research should be focused on the optimization of the working pH range in order to transition from lab scale studies to industrially useful applications. Additionally, the possibility of employing this chitosan-modified MWCNTs-COOH composite for the recovery of other pollutants will also be of notable interest in the field.

Acknowledgments

This work was supported by the State Scholarship Fund sponsored by the China Scholarship Council (Y. H.), National Natural Science Foundation of China (U1612441) (X.L.), Sino-Israeli Intergovernmental Scientific and Technological Cooperation Project (2015DFG92450) (X.L.), Opening Fund of the Skate Key Laboratory of Environmental Geochemistry (SKLEG2016905) (S.D.M.) and the 2014 Cooperative Project Between the Chinese Academy of Sciences and the Xinjiang Autonomous Region (X.L.). The authors would also like to thank the United States National Science Foundation, under award number 1561427 (F.C.M. and S.D.M.) for financial support.

Appendix A. Supplementary data

Supplementary data associated with this article can be found, in the online version, at http://dx.doi.org/10.1016/j.cej.2018.01.133.

References

[1] V.A. Papaevangelou, G.D. Gikas, V.A. Tsihrintzis, Chromium removal from wastewater using HSF and VF pilot-scale constructed wetlands: overall performance, and fate and distribution of this element within the wetland environment, Chemosphere 168 (2017) 716–730.
[2] P. Miretzky, A.F. Cirelli, Cr(VI) and Cr(III) removal from aqueous solution by raw and modified lignocellulosic materials: a review, J. Hazard. Mater. 180 (2010) 1–19.
[3] A.S.K. Kumar, S.-J. Jiang, W.-L. Tseng, Effective adsorption of chromium (VI)/Cr (III) from aqueous solution using ionic liquid functionalized multiwalled carbon nanotubes as a super sorbent, J. Mater. Chem. A 3 (2015) 7044–7057.

[4] S. Parlayici, V. Eskizeybek, A. Avcı, E. Pehlivan, Removal of chromium (VI) using activated carbon-supported-functionalized carbon nanotubes, J. Nanostruct. Chem. 5 (2015) 255–263.
[5] U.S. EPA, Environmental Pollution Control Alternatives: Drinking Water Treatment for Small Communities, EPA Center for Environmental Research Information, 1990.
[6] S. Li, F. Qi, M. Xiao, H. Fan, Y. Shen, K. Du, Z. Zhang, W. Li, In situ synthesis of layered double hydroxides on γ-Al2O3 and its application in chromium (VI) removal, Water Sci. Technol. (2017) wst2017012.
[7] F. Halouane, Y. Oz, D. Meziane, A. Barras, J. Juraszek, S.K. Singh, S. Kurungot, P.K. Shaw, R. Sanyal, R. Boukherroub, Magnetic reduced graphene oxide loaded hydrogels: highly versatile and efficient adsorbents for dyes and selective Cr (VI) ions removal, J. Colloid Interface Sci. 507 (2017) 360–369.
[8] A. Nasrollahpour, S.E. Moradi, Hexavalent chromium removal from water by ionic liquid modified metal-organic frameworks adsorbent, Microporous Mesoporous Mater. 243 (2017) 47–55.
[9] M. Grattieri, N.D. Shivel, I. Sifat, M. Bestetti, S.D. Minteer, Sustainable hypersaline microbial fuel cells: inexpensive recyclable polymer supports for carbon nanotube conductive paint anodes, ChemSusChem 10 (2017) 2053–2058.
[10] S.D. Minteer, B.Y. Liaw, M.J. Cooney, Enzyme-based biofuel cells, Curr. Opin. Biotechnol. 18 (2007) 228–234.
[11] A.J. Bandodkar, J. Wang, Wearable biofuel cells: a review, Electroanalysis 28 (2016) 1188–1200.
[12] F.C. Macazo, D.P. Hickey, S. Abdellaoui, M.S. Sigman, S.D. Minteer, Polymer-immobilized, hybrid multi-catalyst architecture for enhanced electrochemical oxidation of glycerol, Chem. Commun. 53 (2017) 10310–10313.
[13] K. Pillay, E.M. Cukrowska, N.J. Coville, Multi-walled carbon nanotubes as adsorbents for the removal of parts per billion levels of hexavalent chromium from aqueous solution, J. Hazard. Mater. 166 (2009) 1067–1075.
[14] Z. Tian, B. Yang, G. Cui, L. Zhang, Y. Guo, S. Yan, Synthesis of poly (m-phenylenediamine)/iron oxide/acid oxidized multi-wall carbon nanotubes for removal of hexavalent chromium, RSC Adv. 5 (2015) 2266–2275.
[15] M. Alvarez-Rodríguez, M. Alvarez, S. Borragan, F. Martinez-Pastor, W.V. Holt, A. Fazeli, P. de Paz, L. Anel, The addition of heat shock protein HSPA8 to cryoprotective media improves the survival of brown bear (Ursus arctos) spermatozoa during chilling and after cryopreservation, Theriogenology 79 (2013) 541–550.
[16] A. Stafiej, K. Pyrzynska, Adsorption of heavy metal ions with carbon nanotubes, Sep. Purif. Technol. 58 (2007) 49–52.
[17] N.A. Kabbashi, M.A. Atieh, A. Al-Mamun, M.E. Mirghami, M. Alam, N. Yahya, Kinetic adsorption of application of carbon nanotubes for Pb (II) removal from aqueous solution, J. Environ. Sci. 21 (2009) 539–544.
[18] X. Zhao, Q. Jia, N. Song, W. Zhou, Y. Li, Adsorption of Pb (II) from an aqueous solution by titanium dioxide/carbon nanotube nanocomposites: kinetics, thermodynamics, and isotherms, J. Chem. Eng. Data 55 (2010) 4428–4433.
[19] N.M. Bandaru, N. Reta, H. Dalal, A.V. Ellis, J. Shapter, N.H. Voelcker, Enhanced adsorption of mercury ions on thiol derivatized single wall carbon nanotubes, J. Hazard. Mater. 261 (2013) 534–541.
[20] H. Chen, J. Li, D. Shao, X. Ren, X. Wang, Poly (acrylic acid) grafted multiwall carbon nanotubes by plasma techniques for Co (II) removal from aqueous solution, Chem. Eng. J. 210 (2012) 475–481.
[21] C. Lu, C. Liu, F. Su, Sorption kinetics, thermodynamics and competition of Ni 2+ from aqueous solutions onto surface oxidized carbon nanotubes, Desalination 249 (2009) 18–23.
[22] C. Lu, H. Chiu, C. Liu, Removal of zinc (II) from aqueous solution by purified carbon nanotubes: kinetics and equilibrium studies, Ind. Eng. Chem. Res. 45 (2006) 2850–2855.
[23] H.T. Kahraman, Development of an adsorbent via chitosan nano-organoclay assembly to remove hexavalent chromium from wastewater, Int. J. Biol. Macromol. 94 (2017) 202–209.
[24] M. Aliabadi, M. Irani, J. Ismaeili, S. Najafzadeh, Design and evaluation of chitosan/hydroxyapatite composite nanofiber membrane for the removal of heavy metal ions from aqueous solution, J. Taiwan Inst. Chem. Eng. 45 (2014) 518–526.
[25] M.K. Kim, K. Shanmuga Sundaram, G. Anantha Iyengar, K.-P. Lee, A novel chitosan functional gel included with multiwall carbon nanotube and substituted polyaniline as adsorbent for efficient removal of chromium ion, Chem. Eng. J. 267 (2015) 51–64.
[26] H. Beheshti, M. Irani, L. Hosseini, A. Rahimi, M. Aliabadi, Removal of Cr (VI) from aqueous solutions using chitosan/MWCNT/Fe 3 O 4 composite nanofibers-batch and column studies, Chem. Eng. J. 284 (2016) 557–564.
[27] K.W. Jung, T.U. Jeong, M.J. Hwang, K. Kim, K.H. Ahn, Phosphate adsorption ability of biochar/Mg-Al assembled nanocomposites prepared by aluminum-electrode based electro-assisted modification method with MgCl2 as electrolyte, Bioresour. Technol. 198 (2015) 603–610.
[28] J. Hu, C. Chen, X. Zhu, X. Wang, Removal of chromium from aqueous solution by using oxidized multiwalled carbon nanotubes, J. Hazard. Mater. 162 (2009) 1542–1550.
[29] C.-J. Li, S.-S. Zhang, J.-N. Wang, T.-Y. Liu, Preparation of polyamides 6 (PA6)/Chitosan@ Fe x O y composite nanofibers by electrospinning and pyrolysis and their Cr (VI)-removal performance, Catal. Today 224 (2014) 94–103.
[30] D. Park, Y.-S. Yun, J.H. Jo, J.M. Park, Mechanism of hexavalent chromium removal by dead fungal biomass of Aspergillus niger, Water Res. 39 (2005) 533–540.
[31] C.-C. Liu, M.-K. Wang, C.-S. Chiou, Y.-S. Li, Y.-A. Lin, S.-S. Huang, Chromium removal and sorption mechanism from aqueous solutions by wine processing waste sludge, Ind. Eng. Chem. Res. 45 (2006) 8891–8899.
[32] Y. Nakano, K. Takeshita, T. Tsutsumi, Adsorption mechanism of hexavalent chromium by redox within condensed-tannin gel, Water Res. 35 (2001) 496–500.
[33] M.H. Dehghani, M.M. Taher, A.K. Bajpai, B. Heibati, I. Tyagi, M. Asif, S. Agarwal, V.K. Gupta, Removal of noxious Cr (VI) ions using single-walled carbon nanotubes and multi-walled carbon nanotubes, Chem. Eng. J. 279 (2015) 344–352.
[34] J. Hu, G. Chen, I.M.C. Lo, Removal and recovery of Cr(VI) from wastewater by maghemite nanoparticles, Water Res. 39 (2005) 4528–4536.
[35] S.-Y. Wang, Y.-K. Tang, K. Li, Y.-Y. Mo, H.-F. Li, Z.-Q. Gu, Combined performance of biochar sorption and magnetic separation processes for treatment of chromium-contained electroplating wastewater, Bioresour. Technol. 174 (2014) 67–73.
[36] C. Weng, J. Wang, C. Huang, Adsorption of Cr (VI) onto TiO2 from dilute aqueous solutions, Water Sci. Technol. 35 (1997) 55–62.
[37] M.-M. Zhang, Y.-G. Liu, T.-T. Li, W.-H. Xu, B.-H. Zheng, X.-F. Tan, H. Wang, Y.-M. Guo, F.-Y. Guo, S.-F. Wang, Chitosan modification of magnetic biochar produced from Eichhornia crassipes for enhanced sorption of Cr (vi) from aqueous solution, RSC Adv. 5 (2015) 46955–46964.
[38] Y.S. Ho, G. McKay, Pseudo-second order model for sorption processes, Process Biochem. 34 (1999) 451–465.
[39] J. Wang, K. Pan, Q. He, B. Cao, Polyacrylonitrile/polypyrrole core/shell nanofiber mat for the removal of hexavalent chromium from aqueous solution, J. Hazard. Mater. 244 (2013) 121–129.
[40] J. Shang, M. Zong, Y. Yu, X. Kong, Q. Du, Q. Liao, Removal of chromium (VI) from water using nanoscale zerovalent iron particles supported on herb-residue biochar, J. Environ. Manage. 197 (2017) 331–337.
[41] J. Yu, M. Tong, X. Sun, B. Li, Cystine-modified biomass for Cd(II) and Pb(II) biosorption, J. Hazard. Mater. 143 (2007) 277–284.
[42] Ş.S. Bayazit, Ö. Kerkez, Hexavalent chromium adsorption on superparamagnetic multi-wall carbon nanotubes and activated carbon composites, Chem. Eng. Res. Des. 92 (2014) 2725–2733.
[43] M.A. Atieh, Removal of chromium (VI) from polluted water using carbon nanotubes supported with activated carbon, Procedia Environ. Sci. 4 (2011) 281–293.
[44] C. Jung, J. Heo, J. Han, N. Her, S.-J. Lee, J. Oh, J. Ryu, Y. Yoon, Hexavalent chromium removal by various adsorbents: powdered activated carbon, chitosan, and single/multi-walled carbon nanotubes, Sep. Purif. Technol. 106 (2013) 63–71.
[45] R. Kumar, M.O. Ansari, M.A. Barakat, DBSA doped polyaniline/multi-walled carbon nanotubes composite for high efficiency removal of Cr(VI) from aqueous solution, Chem. Eng. J. 228 (2013) 748–755.
[46] L. Li, L. Fan, M. Sun, H. Qiu, X. Li, H. Duan, C. Luo, Adsorbent for chromium removal based on graphene oxide functionalized with magnetic cyclodextrin–chitosan, Colloids Surf., B 107 (2013) 76–83.
[47] G. Sharma, M. Naushad, A.A.H. Al-Muhtaseb, A. Kumar, M.R. Khan, S. Kalia, Shweta, M. Bala, A. Sharma, Fabrication and characterization of chitosan-cross-linked-poly(alginic acid) nanohydrogel for adsorptive removal of Cr(VI) metal ion from aqueous medium, Int. J. Biol. Macromol. 95 (2017) 484–493.
[48] R. Fu, X. Zhang, Z. Xu, X. Guo, D. Bi, W. Zhang, Fast and highly efficient removal of chromium (VI) using humus-supported nanoscale zero-valent iron: influencing factors, kinetics and mechanism, Sep. Purif. Technol. 174 (2017) 362–371.
[49] L. Zhong, X. He, J. Qu, X. Li, Z. Lei, Q. Zhang, X. Liu, Precursor preparation for Ca-Al layered double hydroxide to remove hexavalent chromium coexisting with calcium and magnesium chlorides, J. Solid State Chem. 245 (2017) 200–206.
[50] C. Luo, Z. Tian, B. Yang, L. Zhang, S. Yan, Manganese dioxide/iron oxide/acid oxidized multi-walled carbon nanotube magnetic nanocomposite for enhanced hexavalent chromium removal, Chem. Eng. J. 234 (2013) 256–265.
[51] J. Lu, K. Xu, J. Yang, Y. Hao, F. Cheng, Nano iron oxide impregnated in chitosan bead as a highly efficient sorbent for Cr (VI) removal from water, Carbohydr. Polym. 173 (2017) 28–36.
[52] Z.-N. Huang, X.-L. Wang, D.-S. Yang, Adsorption of Cr (VI) in wastewater using magnetic multi-wall carbon nanotubes, Water Sci. Eng. 8 (2015) 226–232.
[53] M.O. Ansari, R. Kumar, S.A. Ansari, S.P. Ansari, M. Barakat, A. Alshahrie, M.H. Cho, Anion selective pTSA doped polyaniline@ graphene oxide-multiwalled carbon nanotube composite for Cr (VI) and Congo red adsorption, J. Colloid Interface Sci. 496 (2017) 407–415.
[54] C. Luo, R. Wei, D. Guo, S. Zhang, S. Yan, Adsorption behavior of MnO 2 functionalized multi-walled carbon nanotubes for the removal of cadmium from aqueous solutions, Chem. Eng. J. 225 (2013) 406–415.